

10-2009

## SERS in Salt Wells

G. V. Pavan Kumar

*Purdue University - Main Campus*

Joseph Irudayaraj

*Purdue University - Main Campus, josephi@purdue.edu*

Follow this and additional works at: <http://docs.lib.purdue.edu/nanopub>



Part of the [Nanoscience and Nanotechnology Commons](#)

---

Kumar, G. V. Pavan and Irudayaraj, Joseph, "SERS in Salt Wells" (2009). *Birck and NCN Publications*. Paper 488.  
<http://docs.lib.purdue.edu/nanopub/488>

This document has been made available through Purdue e-Pubs, a service of the Purdue University Libraries. Please contact [epubs@purdue.edu](mailto:epubs@purdue.edu) for additional information.

## SERS in Salt Wells

G. V. Pavan Kumar and Joseph Irudayaraj\*<sup>[a]</sup>

We report herein a simple, inexpensive fabrication methodology of salt microwells, and define the utility of the latter as nanoparticle containers for highly sensitive surface-enhanced Raman scattering (SERS) studies. AFM characterization of Ag and Au loaded salt microwells reveal the ability to contain favorable nanostructures such as nanoparticle dimers, which can significantly enhance the Raman intensity of molecules. By performing diffraction-limited confocal Raman microscopy on salt microwells, we show high sensitivity and fidelity in the detection of dyes, peptides, and proteins, as a proof of our concept.

The SERS limit of detection (accumulation time of 1 s) for rhodamine B and TAT contained in salt microwells is 10  $\mu\text{M}$  and 1 nM, respectively. The Raman characterization measurements of salt microwells with three different laser lines (532 nm, 632.81 nm, 785 nm) reveal low background intensity and high signal-to-noise ratio upon nanoparticle loading, which makes them suitable for enhanced Raman detection. SERS mapping of these sub-femtoliter containers show spatial confinement of the relevant analyte to a few microns, which make them potential candidates for microscale bioreactors.

## 1. Introduction

Confining isolated nanoparticles to a small volume is one of the present-day challenges in nanoscience and -technology. The implication of such confinement has tremendous relevance in research aimed at isolated nanoscale chemical and biological reactions in small volumes.<sup>[1,2]</sup> Nanowells have been fabricated via a top-down approach using various sophisticated methods such as focused ion beam milling, electron beam lithography, pulsed laser ablation and so forth.<sup>[1–6]</sup> Although the reliability and versatility of such methods are improving, it still remains an expensive process. An alternate route is to harness the bottom-up approach enabled by chemical self-assembly,<sup>[7,8]</sup> comparatively a less expensive process. In nature too, we observe various living organisms exhibiting spectacular self-assembly via biomineralization<sup>[9,10]</sup> at different scales, which, if mimicked in a laboratory setting, could result in structures not otherwise possible. Various research groups have effectively utilized self-assembly methods to build complicated microscopic and nanoscaled architectures. In recent years, new methods such as template-assisted assembly,<sup>[11]</sup> evaporation-induced assembly<sup>[12]</sup> and many more routes<sup>[7]</sup> have been successfully employed to build materials at different scales. Herein, we describe a simple and inexpensive self-assembly process to construct complex, microscopic rectangular wells for nanoparticles by using a conventional buffer solution with controlled amount of NaCl. We contend that these microarchitectures have the ability to contain isolated and favorable nanostructures such as nanoparticle dimers, which can be exploited to decipher isolated chemical and biological reactions in confined volumes. We harness this simple fabrication method and reveal the utility of Ag and Au nanoparticle-loaded microwells for sensitive, low-volume, high-fidelity detection of biomolecules such as peptides and proteins using surface-enhanced Raman spectroscopy (SERS).

## 2. Results and Discussion

Nanoparticle wells were fabricated on glass slides after being washed with ethanol and water. A specific volume (2  $\mu\text{L}$ ) of buffer solution (2.68 mM of KCl, 1.47 mM of  $\text{KH}_2\text{PO}_4$  and 8.1 mM of  $\text{Na}_2\text{HPO}_4$ ) with 137 mM of NaCl solution (1  $\mu\text{L}$ ) was drop-casted onto the slides. All of the abovementioned chemicals also serve as components of a biological buffer (phosphate buffer saline, PBS), and hence their utility is two-fold. After 10 min, 1  $\mu\text{L}$  of the desired nanoparticle solution was introduced to the drop-casted liquid and the mixture was left to dry at normal (room) temperature and pressure. After 30 min, gradual growth of rectangular and square crystals (5 to 10  $\mu\text{m}$  in length) of the buffer salt was observed as the solvent in the mixture evaporated. It should be noted that the two- (Figure 1 a) and three- (Figure 1 b) dimensional AFM images of a nanoparticle well reveal a trough at the center of all such salt structures formed. The depth of the trough at the center of

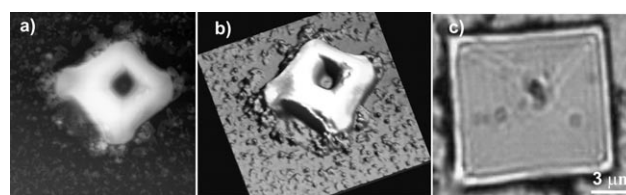


**Figure 1.** a) 2D and b) 3D AFM images of nanoparticle wells. The scan size is 15  $\mu\text{m} \times 15 \mu\text{m}$ , c) Bottom-illuminated optical image of a container formed on a glass slide.

[a] Dr. G. V. P. Kumar, Prof. J. Irudayaraj  
Birck Nanotechnology & Bindley Bioscience Center  
Agricultural & Biological Engineering, Purdue University  
225 S. University Street, West Lafayette, IN 47906 (USA)  
Fax: (+1) 765-496-1115  
E-mail: josephi@purdue.edu

Supporting information for this article is available on the WWW under <http://dx.doi.org/10.1002/cphc.200900634>.

the crystal was estimated as  $2\ \mu\text{m}$  (see Section S1 in the Supporting Information). Some of the crystals exhibited inverse-pyramid-shaped troughs, with a flat apex at the center. If the shape of the trough is approximated as an inverse square pyramid, the calculated volume of such a container was  $\sim 0.055\ \text{fL}$  (see Section S1 in the Supporting Information). Note that the AFM image of microwells without nanoparticle loading did not exhibit any protrusions from the trough region (see AFM image in Figure S1a of the Supporting Information). Further, the optical microscopic image of numerous salt microwells formed over a large surface area revealed consistency in terms of shape and morphology (see Figure S1b in the Supporting Information). Although the AFM image clearly showed a trough at the center of the container, the optical image in Figure 1c provides the initial cues to its presence. The central part of the structure shows a darker contrast corresponding to the trough, which acts as a container in the optical image. In order to test the formation of such a complex structure on a different platform, the above fabrication was repeated on a cleaned silicon wafer, and the same type of geometrical formation was observed (see Section S2 in the Supporting Information). It is important to note that the concentration of NaCl was extremely important in the formation of these containers. A higher concentration ( $> 200\ \text{mM}$ ) of NaCl leads to crystals of arbitrary shapes, and hence is not desirable.

Having observed the trough formation at the center of the microwells (also denoted as microcontainers), further characterization of this region was done with high-resolution atomic force microscopy. Figures 2a and b show the AFM image of a nanoparticle container at two different magnifications. Figure 2b is the zoomed-in image of the central part of the trough. We observed well-separated, individual nanoparticles residing at the trough of the container. A closer examination reveals that the central part of the trough has small strips of depletions in which most of the individual nanoparticles reside. To

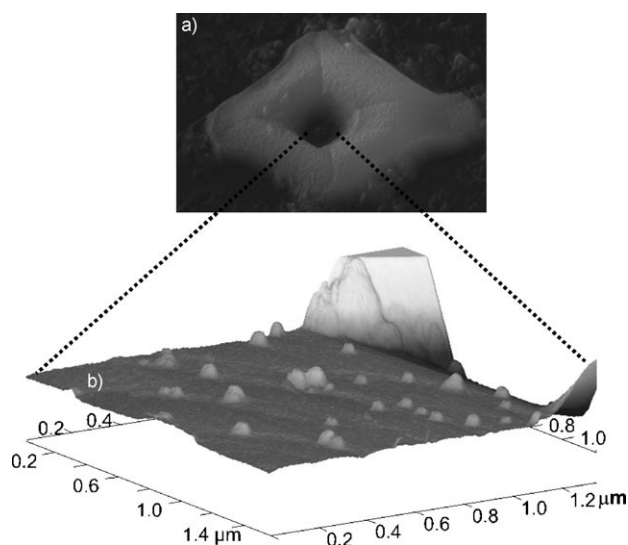


**Figure 2.** a) Low-magnification AFM image of a nanoparticle well (scan size:  $15\ \mu\text{m} \times 10\ \mu\text{m}$ ). b) Zoomed-in AFM image of the base of this well. Isolated nanoparticles are clearly evident in (b).

further test the assembly of such nanoparticles (with Ag nanoparticle, Ag NPs) in the trough, two-dimensional AFM images (see Section S3 in the Supporting Information) were obtained and analyzed. Assembly of Ag nanoparticle dimers on the surface was clearly observed (see Section S3 in the Supporting Information). In recent times, metallic nanoparticle dimers have derived great interest among researchers because of the enhanced optical fields created at the junction of these dimers, which act as SERS hot-spots due to plasmon coupling. Any molecule that resides in a hot-spot can be detected with high sensitivity as shown in the recent reports by Xia and coworkers.<sup>[13,14]</sup> In addition, all the Ag dimers formed on the surface had a size mismatch, as one of the particles was always slightly larger than the other (see Section S3 in the Supporting Information). Also, the height contrast (in Section S3 in the Supporting Information) indicates that base of the trough is not perfectly flat, but may have undulations at the nanoscale. The same measurement was also performed on salt microwells loaded with Au nanoparticles, and presented by the AFM images showing isolated nanoparticles including dimers (see Section S4 in the Supporting Information).

As a potential application of our nanoparticle wells produced by the described method, we show their utility in surface-enhanced Raman spectroscopy (SERS). To characterize the containers, Raman control measurements of salt structures (without nanoparticle loading) at three different Raman excitation wavelengths: 532 nm, 632.81 nm, and 785 nm were performed. The background signals for all of the excitation wavelengths were weak (see Section S5 in the Supporting Information). Next, with the assistance of an optical microscope, a small volume of relevant analyte to be detected ( $< 0.1\ \mu\text{L}$ ) was microinjected by a syringe over the salt structures pre-loaded either with Ag or Au nanoparticles. After 10 min, the laser was focused at the trough of the nanoparticle container to retrieve the SERS spectra. Figures 3a,b show two examples of high signal-to-noise ratio SERS spectra obtained from rhodamine B (rB) and TAT peptide deposited in the Ag nanoparticle containers, respectively. The concentration of rB and TAT were  $0.01\ \mu\text{M}$  and  $1\ \mu\text{M}$ , and the signal accumulation times were 1 sec and 10 sec, respectively. The inset in Figure 3a shows an optical image of a nanoparticle well loaded with rB dye. A reddish tinge from the dye was observed at the center of all such containers. Also, shown in the inset of Figure 3b is the optical image of a TAT-peptide-loaded nanoparticle container. We observed bright, white lines converging towards the center of the trough after the peptide solution was loaded. In order to substantiate the role of microwells as nanoparticle containers, the SERS signals of rB were compared to conventional SERS substrate (i.e. nanoparticle on glass surface). The intensity of Raman signal from the former case was three orders of magnitude greater than the conventional substrates (see Figure S5b in the Supporting Information).

The SERS limit of detection of rB molecules using nanoparticle containers loaded with Ag was  $10^{-11}\ \text{M}$  (see Section S6 in the Supporting Information). By performing surface-enhanced resonant Raman measurements with the laser excitation at 532 nm, which is in resonance with the electronic transition of

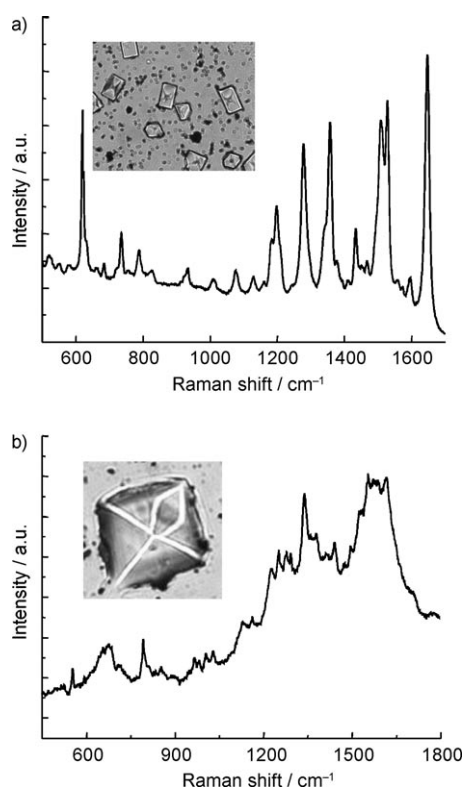


**Figure 3.** a) SERS spectrum of rhodamine B captured from the nanoparticle well, b) SERS spectrum of TAT peptide in a nanoparticle well. The signal accumulation times for (a) and (b) were 1 and 10 s, respectively. The inset shows an optical image of nanoparticle wells filled with relevant molecules.

rB molecules, the limit of detection of rB could be increased by an order of magnitude (see Section S6 in the Supporting Information).

In order to reveal the sensitivity of our detection method, we efficiently detected a low Raman cross-section protein, BSA at micro molar concentration (see Section S7 in the Supporting Information) using the nanoparticle containers loaded with Ag and Au nanoparticles. To confirm the band structure of the resultant spectra, SERS of BSA with Ag nanoparticle on glass was recorded (see Figure S72 in the Supporting Information). We observed a good correspondence between the SERS in salt microwells and nanoparticles on glass, which confirm the utility of these structures for biomolecular detection.

To test the spatial confinement of the molecules within the trough of nanoparticle containers, Raman imaging was performed in wells with rB-loaded Ag nanoparticles (Figure 4). The data in Figure 4a is the SERS map of  $1648\text{ cm}^{-1}$  band of rB collected with a laser dwell time of 1 s per spot. Figure 4b shows the corresponding optical image of the mapped microwell. The SERS signal from the trough of the container was clearly evident from Figure 4a, and indicates that rB is spatially confined to the trough of the microcontainer. Our results clearly reveal that nanoparticle-loaded salt microcontainers can indeed be used for highly sensitive, low-volume, molecular detection using SERS.

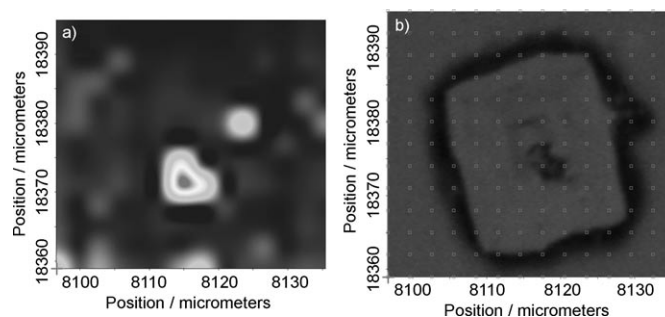


**Figure 4.** a) Raman image of the  $1648\text{ cm}^{-1}$  band of a rhodamine B molecule loaded inside an Ag nanoparticle container. b) The corresponding optical image of the nanoparticle well shows mapped points.

### 3. Conclusions

In summary, a simple and inexpensive method to produce microscaled nanoparticle wells is outlined. Individual nanoparticles assemble at the trough of the container to form dimers and other configurations. The containers loaded with Ag and Au nanoparticles exhibit SERS properties, and are sensitive to biomolecular detection at low concentrations. By periodically assembling the containers in the form of an array, its utility could be expanded to construct biocompatible, soft-material platforms for optically assisted proteomics and genomics. Further research in controlling the morphology and size of these wells are underway, as these show immense promise in achieving isolated nanoscale bio-reactors.

### Experimental Section

All chemicals were purchased from Sigma Aldrich (USA). Atomic Force Microscope (AFM) images were acquired using the BioScope II from Veeco, mounted on an Olympus IX-71 inverted microscope and equipped with the NanoScope V controller. Imaging was performed using the tapping mode in air at scan rates between 0.6–1.0 Hz with an image resolution of  $256 \times 256$  pixels. AFM image processing and analysis was performed using WSxM software, whose details can be found elsewhere.<sup>[15]</sup> Surface-enhanced Raman spectroscopy measurements were performed using the Bruker Senterra confocal Raman microscope. For the present work, we have utilized three different Raman excitation sources: 532 nm, 632.81 nm and 785 nm. Optical images were captured with the camera attached to the Raman microscope. Citrate-reduced Ag and Au nanoparticles were produced by the Lee and Meisel method.<sup>[16]</sup> Further details on nanoparticle synthesis and size can be found in Section S8 of the Supporting Information. Field-emission scanning electron microscope images are included in Section S9 of the Supporting Information to substantiate the AFM observations.

### Acknowledgements

We acknowledge Waranatha Abeygunasekara and Dr. Helen A. McNally of the Department of Electrical and Computer Engineering Technology and the Bindley Biosciences Center, Purdue University for assistance in AFM imaging.

**Keywords:** microwells · nanoparticles · Raman spectroscopy · salt crystals · self-assembly

- [1] Y. Rondelez, G. Tresset, K. V. Tabata, H. Arata, H. Fujita, S. Takeuchi, H. Noji, *Nat. Biotechnol.* **2005**, *23*, 361.
- [2] D. T. Chiu, C. F. Wilson, F. Ryttsen, A. Stromberg, C. Farre, A. Karlsson, S. Nordholm, A. Gaggar, B. P. Modi, A. Moscho, R. A. Garza-Lopez, O. Orwar, R. N. Zare, *Science* **1999**, *283*, 1892.
- [3] J. E. Barton, T. W. Odom, *Nano Lett.* **2004**, *4*, 1525.
- [4] R. J. Jackman, D. C. Duffy, E. Ostuni, N. D. Willmore, G. M. Whitesides, *Anal. Chem.* **1998**, *70*, 2280.
- [5] N. S. John, N. R. Selvi, M. Mathur, R. Govindarajan, G. U. Kulkarni, *J Phys Chem. B* **2006**, *110*, 22975.
- [6] H. Chun, M. G. Hahm, Y. Homma, R. Meritz, K. Kuramochi, L. Menon, L. Ci, P. M. Ajayan, Y. J. Jung, *ACS Nano* **2009**, *3*, 1274.
- [7] G. M. Whitesides, B. Grzybowski, *Science* **2002**, *295*, 2418.
- [8] Z. R. R. Tian, J. Liu, J. A. Voigt, B. McKenzie, H. F. Xu, *Angew. Chem. Int. Ed.* **2003**, *42*, 414; *Angew. Chem.* **2003**, *115*, 429.
- [9] H. Cölfen, S. Mann, *Angew. Chem. Int. Ed.* **2003**, *42*, 2350; *Angew. Chem.* **2003**, *115*, 2452.
- [10] D. Philp, J. F. Stoddart, *Angew. Chem. Int. Ed. Engl.* **1996**, *35*, 1154; *Angew. Chem.* **1996**, *108*, 1242.
- [11] Y. Yin, Y. Lu, B. Gates, Y. Xia, *J. Am. Chem. Soc.* **2001**, *123*, 8718.
- [12] C. J. Brinker, Y. Lu, A. Sellinger, H. Fan, *Adv. Mater.* **1999**, *11*, 579.
- [13] W. Li, P. H. C. Camargo, X. Lu, Y. Xia, *Nano Lett.* **2009**, *9*, 485.
- [14] P. H. C. Camargo, M. Rycenga, L. Au, Y. Xia, *Angew. Chem. Int. Ed.* **2009**, *48*, 2180; *Angew. Chem.* **2009**, *121*, 2214.
- [15] I. Horcas, R. Fernandez, J. M. Gomez-Rodriguez, J. Colchero, J. Gomez-Herrero, A. M. Baro, *Rev Sci Instrum* **2007**, *78*, 013705.
- [16] P. C. Lee, D. Meisel, *J Phys Chem.* **1982**, *86*, 3391.

Received: August 10, 2009

Published online on September 11, 2009